

# Effect of Electrode Coating Type on the Physico-chemical Properties of Slag and Welding Technique

**Abstract:** The article presents the results of the physico-chemical tests concerning the properties of various slags formed after welding with low-hydrogen and rutile electrodes as well as flux-cored wires. The slags tested were analysed for their phase compositions using X-ray diffractometry (XRD) X-ray fluorescence (XRF). The behaviour of slags at temperatures elevated to 1400°C was examined using a high-temperature microscope. The analysis of the high-temperature tests enabled the determination of slag characteristic temperatures, i.e. softening and melting points. The results obtained demonstrated various properties of slags, with the lowest characteristic temperatures for low-hydrogen slags and the highest characteristic temperatures for flux-cored wire slags. In addition, on the basis of different characteristic temperatures slags were classified in relation to their solidification rates.

**Keywords:** low-hydrogen electrodes, rutile electrodes, flux-cored wires, slag properties

## Introduction

Welding using covered electrodes and flux-cored wires is an important and indispensable technique while performing welding processes in construction site conditions. Slag formed during welding by means of these methods protects a weld pool against oxidation, stabilises arc burning, ensures the proper chemical composition of a weld and provides the insulation protection thereof (Fig. 1). The type and chemical composition of coatings significantly affect the mechanical strength of a weld. In addition, the physical properties of solid-state and liquid state coatings, such as grain size, viscosity, surface tension, thermal expansion coefficient and heat capacity also influence the obtainment of a good quality weld in a required shape [1-6].

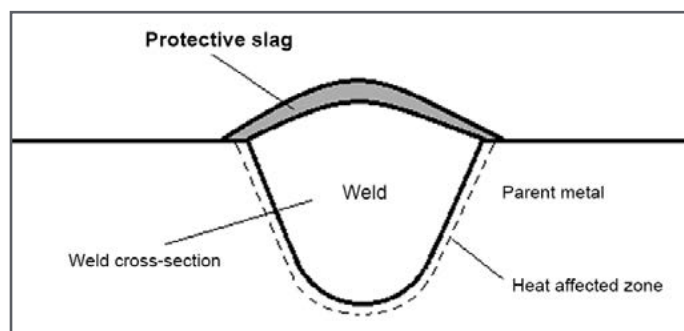


Fig. 1. Weld in cross-sectional view

The production of covered electrodes is a multi-stage process (see Fig. 2).

The first and most important issue in the production of covered electrodes is the chemical composition of the coating mixture. The various behaviours of mixtures and fluxes available on the market depend on their chemical

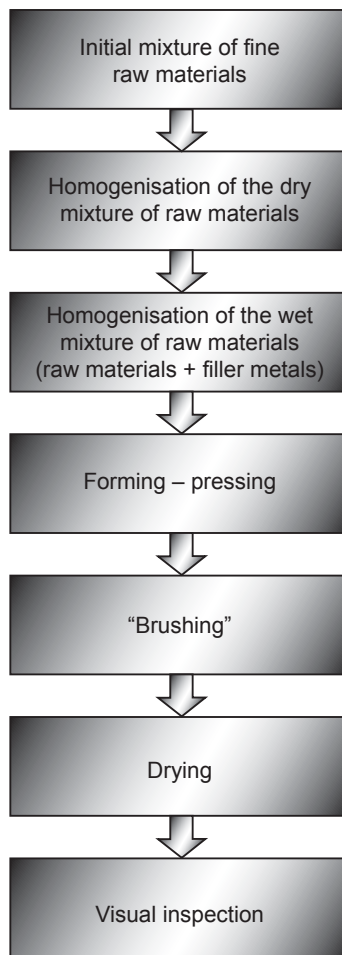
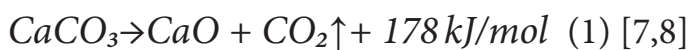


Fig. 2. Simplified production scheme of covered electrode production

composition, the geological origin of the raw materials used for their production and the manufacturing process itself [1]. The selection of raw materials for the preparation of a coating depends on the required phase composition of a dry mixture. Having the foregoing in view, such a dry mixture should contain minerals, which during welding, release gases stabilising an arc and protecting the liquid weld pool. The most commonly used minerals providing gaseous protection include calcite, supplied with limestone, having a chemical formula of  $\text{CaCO}_3$ . The thermal decomposition of  $\text{CaCO}_3$  takes place at  $950^\circ\text{C}$ , leading to the formation of  $\text{CaO}$  and  $\text{CO}_2$  (1), which, in turn decomposes (in arc plasma) into carbon monoxide and atomic oxygen in accordance with the reactions (2, 3) [7]:



The reaction of carbonate decarbonisation is endothermic in nature. In this reaction, released  $\text{CO}_2$  makes up 44% of the total calcite mass. The transport of  $\text{CO}_2$  takes place as a result of Knudsen diffusion through voids and cracks between phases and through spaces formed due to the separation of  $\text{CaO}$  crystals from  $\text{CaCO}_3$  not yet decomposed [8]. J.D. Plessis and the co-authors [9] examined the effect of calcium carbonate content in the phase composition of a low-hydrogen coating mixture on the content of hydrogen diffusing in a weld metal, with calcite content in the mixture varying between 10% and 24%. Tests revealed a decreasing amount of hydrogen in a weld for mixtures containing up to 18% of  $\text{CaCO}_3$ . Greater  $\text{CaCO}_3$  amounts produced the opposite effect.

While preparing coating mixtures it is also possible to use a number of other carbonates (Table 1), yet they are used to a lesser degree. As can be seen in Table 1, the mineral releasing the greatest amount of  $\text{CO}_2$  is magnesite, whilst iron carbonate (siderite) decomposes releasing the smallest amount of the above mentioned gaseous compound. It should be emphasized that among all basic oxides it is calcium oxide that has the greatest ability to absorb and fix water in the structure, hence its excellent capability of reducing hydrogen and oxygen contents in a molten metal area. The ability of magnesium

Table 1. Minerals containing the carbonate group ( $\text{CO}_3^{2-}$ ), the products of their thermal decomposition and the amounts of  $\text{CO}_2$  released in a decarburisation reaction [3,4].

Mineral	Thermal decomposition products	Amount of released $\text{CO}_2$ , % by weight
calcite – $\text{CaCO}_3$	$\text{CaO}, \text{CO}_2$	44.0
magnesite – $\text{MgCO}_3$	$\text{MgO}, \text{CO}_2$	52.2
siderite – $\text{FeCO}_3$	$\text{FeO}, \text{CO}_2$	38.0
dolomite – $\text{CaMg}(\text{CO}_3)_2$	$\text{MgO}, \text{CaO}, \text{CO}_2$	47.7

oxide to react with water is significantly inferior if compared with that of CaO, which is additionally responsible for the predominant popularity of calcium carbonate [10-16].

The thermal decomposition of magnesite and that of siderite are similar, in accordance with the reaction (1). In turn, dolomite decomposes in a two-stage reaction. During the first stage, at a temperature of 700-750°C, reaction products are CaCO<sub>3</sub>, MgO and CO<sub>2</sub>. The second stage takes place at a temperature of 900-1000°C and leads to the decomposition of CaCO<sub>3</sub> into CaO and CO<sub>2</sub> [16]. It should be mentioned that the greater the carbonate fraction, the higher the basicity of slag and the lower the hydrogen content in a weld [9]. This is due to a greater tendency to fix water in a structure through the absorption of hydrogen from arc plasma, which prevents the hydrogen from entering a liquid metal.

Other raw materials used in the production of coatings include clays containing aluminium silicates e.g. kaolinite – Al<sub>4</sub>Si<sub>4</sub>O<sub>10</sub>(OH)<sub>8</sub>, alkaline feldspars containing aluminosilicates such as orthoclase (KAlSi<sub>3</sub>O<sub>8</sub>) and albite (NaAlSi<sub>3</sub>O<sub>8</sub>), quartzites enriched in silicon dioxides (96-98 % mol.) and high-purity titanium dioxide containing over 95% TiO<sub>2</sub>. The third group is composed of ferroalloys supplied to a mixture in order to deoxidise a liquid metal in a weld. Ferromanganese (FeMn), ferrotitanium (FeTi) and ferrosilicon (FeSi) belong to the group of deoxidising raw materials most commonly used for the preparation of coating mixtures and fluxes. The addition of fine iron (Fe) enables faster melting of the electrode, thus increasing welding process efficiency. Welding without the aforesaid component requires greater power consumption, is responsible for a droplet-type liquid metal transport mode (more difficult to control) and leads to a greater number of spatters [18].

The appropriate fluidity of molten slag and the reduction of diffusive hydrogen content are obtained by adding components containing fluoride ions [9]. Calcium fluoride, CaF<sub>2</sub>, is most

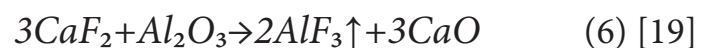
commonly used in the production of coating mixtures and is provided in the form of fluorite (melting point 1418°C). As the low-hydrogen (basic) components of mixtures are characterised by a greater ability to fix water, CaF<sub>2</sub> is commonly used in the production of low-hydrogen (basic) electrodes. Tests conducted by C.S. Chai and co-authors [18] revealed that fluorine, F<sub>2</sub>, reacts with hydrogen molecules forming hydrogen fluoride, HF, in accordance with the reaction (4):



Hydrogen fluoride does not dissolve in liquid iron and evaporates from an arc area [9]. Sadly, calcium fluoride is not sufficiently active and its part enters slag. Therefore, it seems advisable to investigate the behaviour of other fluorides. It has been found that calcium fluoride in the presence of silicon dioxide, SiO<sub>2</sub>, reduces its oxidising ability forming silicon fluoride, SiF<sub>4</sub>, as can be seen in the reaction (5):



During submerged arc welding it is possible to observe the formation of a small amount of silicon fluoride which decreases the partial pressure of hydrogen. In addition, it has been found that the formation of SiF<sub>4</sub> does not reduce the content of silicon in a weld [18]. T. Lau and co-authors [19] noticed the reaction between calcium fluoride and aluminium oxide in slag, in accordance with the equation (6):



Fluorite is entirely included in the slag ratio, expressed by a basic component – acidic component ratio in accordance with the equation (7), describing the metallurgical behaviour of a coating mixture and having a significant effect on the toughness of a weld [12]. The higher the basicity, the lower the hydrogen content in a weld and the greater the toughness of a weld [12,20].

$$B_I = (CaO + MgO + BaO + SrO + Na_2O + K_2O + Li_2O + CaF_2 + 0,5 \cdot (MnO + FeO)) / (SiO_2 + 0,5 \cdot (MnO + FeO)) \quad (7) \quad [20]$$

H. Terashima and co-authors [21] have observed a decrease in the content of hydrogen diffusing in a weld from 12 to 2ml per 100g of molten metal with a slag ratio increasing from 0 to 3 respectively. It has been established that the type of oxide present in a coating mixture affects the ease of slag separation from the surface of a weld. The presence of calcium fluoride is responsible for the difficult separation of slag, similarly as in the case of cordierite –  $Mg_2Al_3[AlSi_5O_{18}]$  and the solid solution of spinel ( $Mg, Mn, Cr$ )  $O \cdot (Al, Cr, Mn)_2O_3$ . Slag behaves otherwise in cases of increased amounts of  $SiO_2$ ,  $Al_2O_3$  and  $Cr_2TiO_2$ , the presence of which facilitates the separation of slag [1].

The chemical composition and the physico-chemical properties of a coating mixture, dependent on the raw material used, have a significant influence on the penetration depth [1,22]. T.H. Hazzlet [23] noticed that the presence of pure  $CaCO_3$ ,  $K_2CO_3$  and  $CaF_2$  causes shallow penetration, whereas  $Na_3CO_3$ ,  $MnO_2$ ,  $Al_2O_3$ ,  $SiO_2$  and  $MgO$  lead to the obtainment of a medium depth of penetration. It has also been found that the presence of  $MgCO_3$  in a coating mixture ensures the obtainment of deep penetration.

Binding agents constitute another important group of components used in the production of coating mixtures applied exclusively for manufacturing covered electrodes as they provide the sufficient strength of a mixture during and after the process of formation. The solutions of sodium and potassium silicates ( $M_a(SiO_2)_bO$ , where  $M=Na^+$  or  $K^+$ ) are used mainly as filler metals. This group of chemical compounds affects the centricity of a covered electrode, being a precondition for stable arc burning and proper weld formation, particularly while making root runs [18]. The addition of carboxymethylcellulose or cellulose (in low-hydrogen and rutile electrodes respectively) as a plasticiser

prevents the excessively fast drying of a mixture, which could trigger the formation of cracks on a coating surface. Plasticisers of graining below 0.3 mm are used in small amounts (approximately 0.5-1%) as additions to mixtures [24]. A coating is pressed by a set of nozzles, uniformly covering a wire. The precise control of nozzle alignment is of crucial importance for the obtainment of uniformly covered electrodes. After pressing, covered electrodes undergo heat treatment.

The process of heat treatment depends on the chemical composition of an electrode and is conducted at various temperatures in a one or two-stage process, depending on the type of electrode:

- rutile electrodes – one-stage drying (approximately 105°C),
- low-hydrogen (basic) electrodes – two-stage drying 1: 100°C, 2: 420-450°C).

The first stage of drying aims to remove hygroscopic water, whereas the second stage of the heat treatment of low-hydrogen electrodes is connected with the fact that basic compounds are characterised by significant water absorption and hydration tendency [24]. During the heat treatment of electrodes the gases formed as a result of the reaction between ferroalloys (particularly FeSi) and sodium silicate can impede the drying process and increase crack formation susceptibility. For this reason, the traditional addition of fine FeSi to a mixture has been replaced by the addition of FeSi produced in the process of spraying. The particles of sprayed ferroalloy are covered with a thin layer of silicon oxide and, as a result, are less susceptible to reacting with sodium silicate.

The objective of this study is to determine the physico-chemical behaviour of various types of slag specimens formed during welding with vertical upwards progression (PF), using various welding consumables available on the market, as well as to assess their impact on a welding technique.

## Materials and Methods

The study-related tests involved the use of several types of electrodes available on the market, i.e. three grades of low-hydrogen electrodes and three grades of rutile electrodes. In addition, the tests also included one grade of a rutile flux-cored wire. The characteristics of the materials tested are presented in Table 2. Welds were made of S355J2+N steel in vertical upwards progression (PF) (in accordance with EN 10025-2) [25,26]. The diameter of the electrodes and rutile flux-cored wire used amounted to 3.2 mm and 1.2 mm respectively. Welding current adjusted for the electrodes amounted to 100 A and that for the flux cored wire was 190 A. During the tests involving the flux cored wire the shielding gas used was a mixture composed of 80% Ar and 20% CO<sub>2</sub> (M21). Slag specimens were sampled from the welds and designated as presented in Table 2.

Table 2. Characteristics of materials used in the tests

Material/ welding method	Producer	Electrode designation	European electrode designation	Slag designation
Low-hydrogen electrodes/ 111	Oerlikon	Special	E 38 3 B 12 according to EN ISO 2560-A	BO
	Esab	EB146	E 38 3 B 42 according to EN ISO 2560-A	BE
	Metalweld	EVB47	E 42 2 B 32 according to EN ISO 2560-A	BM
Rutile electrodes/ 111	Oerlikon	Overcord	E 38 0 R 12 according to EN ISO 2560-A	RO
	Esab	ER146	E 38 0 R 12 according to EN ISO 2560-A	RE
	Metalweld	Rutweld 13	E 38 0 R 12 according to EN ISO 2560-A	RM
Flux-cored wire/ 136	Nittetsu	SF-3AM	T 46 4 Z P M 2 H 5 according to EN ISO 17632-A	FCW

The slag specimens sampled were subjected to a phase analysis using an X-ray diffractometer (XRD; X'Pert Pro by Philips) in the range of angles 2 theta 5-90°, applying radiation Cu K<sub>α</sub> (λ=1,54056 Å) and to chemical element analysis using X-ray fluorescence (XRF; Philips X'Unique II). The specimens were also examined using a high-temperature microscope at a temperature of 1400°C and a heating rate of 10°C/min.

Table 3. Chemical element analysis of slag specimens

Specimen	Chemical element content, % by weight											
	O	Ca	Si	Mg	Ti	Mn	Fe	K	Na	Al	Cr	F
<b>Low-hydrogen slag</b>												
BO	37.2	23.4	16.7	1.6	3.1	7.1	6.1	1.8	0.2	0.6	0.1	2.1
BE	32.2	32.7	10.2	0.1	5.9	4.6	2.8	0.9	0.9	0.5	0.03	9.2
BM	31.9	31.2	8.9	0.3	8.6	3.9	4.1	1.3	0.1	0.4	0.04	9.3
<b>Rutile slag</b>												
RO	38.6	3.6	9.7	0.1	24.3	8.5	8.3	3.1	0.7	3	0.1	-
RE	38.3	3.8	8.3	0.1	25.9	10.1	8.1	1.1	1.7	2.5	0.1	-
RM	39.7	2.4	9.5	0.1	26.3	8.1	6.6	3.2	0.3	3.7	0.1	-
<b>Flux-cored wire slag</b>												
FCW	37	0.1	2.3	4.7	37.7	11.9	1.5	0.2	1.8	1.3	0.04	1.5

## Results and Discussion

Table 3 presents the chemical element analysis of the slag specimens conducted using the XRF method. As can be seen, the chemical compositions of the BE and BM slags are similar. The contents of the main elements such as Ca, Si, Ti and Mn are similar in the BE and BM slags. In turn, the BO slag contains less Ca and Ti and more Si and Mn. The chemical composition of the rutile electrodes tested is similar. The FCW slag is characterised by smaller amounts of Si and Ca and greater amounts of Mg, Ti and Mn if compared with the slag obtained from the rutile electrodes.

Figure 3 presents the results of the low-hydrogen slag XRD analysis. The diffraction patterns of the BE and BM specimens reveal their multi-phase nature. The diffraction pattern of the BO specimen presents a strongly amorphous structure, resulting from a greater fraction of a silicate phase having undergone fast cooling-induced vitrification. The diffraction pattern of the BO specimen is typical of compounds having an amorphous structure. In order to provide better characteristics and understand the BO slag “behaviour”, conducting additional tests, e.g. employing infrared spectroscopy (IR), seems highly advisable. The diffraction patterns of the BE and BM specimens contain reflexes characteristic of fluoroite, silicates and titanates as well as a high-intensity reflex originating from rutile at  $2\theta=27.52^\circ$  (BE specimen) and at  $2\theta=27.39^\circ$  (BM specimen). Similar phases were previously recorded in relation to post-weld slag by C.T. Vaza and co-authors [4]. In addition, the diffraction pattern of the BM slag is characterised by a greater amount of higher intensity reflexes for calcium titanate  $\text{CaTiO}_3$ .

The equilibrium in a pyrometallurgical reaction is known to be difficult

to achieve due to a high temperature, density gradient, very fast heat transfer from an arc and a significant number of various slag and metal phases. The thermodynamic equilibrium of a welding process is obtained only locally in small volumes, at high temperatures and for a high area to volume ratio. For this reason, it is necessary to act prudently while using equilibrium conditions [14]. The presence of other phases in the composition of slag cannot be excluded, yet their amount can be below the XRD method limit of detection or such phases may be not fully ordered.

The main phase in the rutile electrode slag (RO, RE, RM) composition is  $\text{Fe}_2\text{MnTi}_3\text{O}_{10}$  of orthorhombic symmetry (Fig. 4). All the specimens, tested using XRD, also revealed the presence of iron titanate  $\text{FeTiO}_3$  having the structure of perovskite. The XRD diffraction pattern of the flux-cored wire (FCW) slag is analogous to that of the rutile electrode slag. Slight displacements in reflex positions in both phases can be attributed

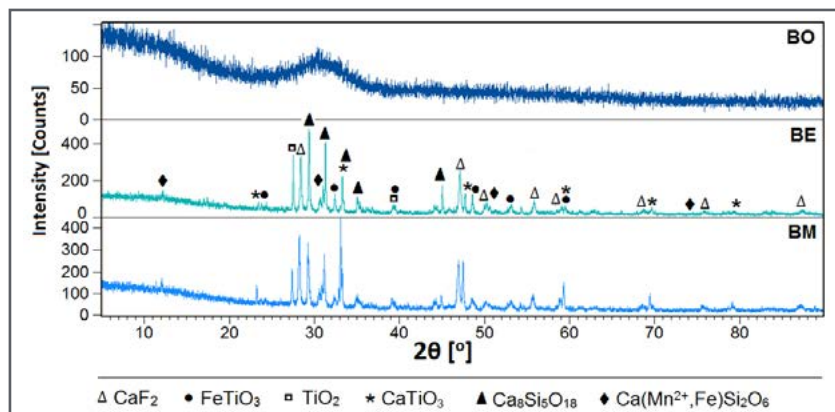


Fig. 3. Diffraction patterns of low-hydrogen electrode (BO, BE, BM) slags

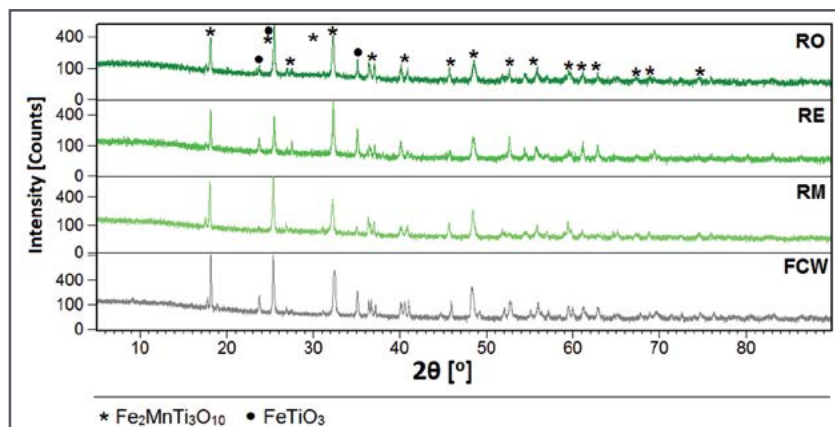


Fig. 4. Diffraction patterns of (RO, RE, RM) rutile electrode slags and flux-cored wire (FCW) slag

to the isovalent and heterovalent substitution of iron ions with magnesium ions ( $Mg^{2+} \leftrightarrow Fe^{2+/3+}$ ) present in the slag, due to a very small difference in their electronegativity in the electrochemical series and ionic radiuses ( $r_{Mg^{2+}}=0.072$  nm,  $r_{Fe^{2+}}=0.078$  nm,  $r_{Fe^{3+}}=0.065$  nm) (Table 3).

The selected characteristic temperatures of the slag specimens tested, such as softening and melting points, were determined by observing the changes of specimen shapes during high-temperature microscopic observations. The characteristic values of slag temperature are presented in Table 4. The photographs for the BO specimen softening and melting points are presented in Figure 5. It was observed that the BO low-hydrogen slag had lower softening and melting points. Such a behaviour can be ascribed to the significant amount of the amorphous phase, detected using the XRD method (Fig. 3, BO). The microscopic observations also revealed a small temperature range (approximately 30°C) between the softening and melting points (Fig. 5). The specimen started to soften at 1100°C and was entirely molten at 1130°C. The BO slag melting point is lower by approximately 85°C than the softening points of the BE and BM slags. As a result, welding by means of BO electrodes makes it possible to use lower welding parameters with simultaneously maintaining electrode melting stability. The small temperature range between the softening and melting point and high viscosity, caused by an increased amount of silicates (Table 3, Fig. 3-BO) prevent the outflow of slag and the fall of liquid metal making welding in difficult positions, such as PF, PE, PD or PG, significantly easier. In addition, the low solidification point of the slag enables the release of gases from a weld and is responsible for lower weld porosity. During the microscopic examination of the BM specimen it was possible to observe the release of residual gases from the slag at a temperature of

900°C. The thermal behaviour of the BE and BM specimens is similar, the effect of which will be their similar behaviour during welding and the obtainment of similar quality welds. The low melting point of low-hydrogen slag imposes the necessity of using a short arc welding technique, which will also protect the weld pool against overheating [6,25-29].

The observation of the rutile slags revealed their higher softening and melting points if compared with those of low-hydrogen slags. Significantly higher melting points of rutile slags enable the obtainment of high-quality welds using long-arc welding techniques [30]. However, high solidification points of rutile slags can confine residual gases in a weld, possibly leading to its increased porosity and reduced mechanical strength [26].

The FCW slags are characterised by the highest softening and melting points and a relatively small temperature range of 40°C between these points, indicating the fast solidification of the slag. The fast FCW slag solidification prevents the weld pool from hanging down. As a result, electrodes can be used for welding positions considered as difficult (PF and PG) and at higher welding parameters, which increases welding process efficiency [31]. The melting point of the FCW specimen is higher than that of any other rutile slags, probably due to higher contents of magnesium and manganese ions built-in in the crystalline structure of the FCW slag specimen. During the tests it was observed that

Table 4. Results of observations using a high-temperature microscope

Slag designation	Softening point, °C	Melting point, °C	Temperature range between the melting and softening points, °C
BO	1100	1130	30
BE	1170	1200	30
BM	1200	1230	30
RO	1160	1260	100
RE	1150	1240	90
RM	1200	1270	70
FCW	1360	1400	40

the FCW welding parameters are almost twice as high if compared with welding using a covered electrode in the same welding position.

## Conclusions

The research involved welding tests in vertical upwards progression using electrodes provided with low-hydrogen and rutile coatings as well as using flux-cored wires. Slags collected from a surface welded were subjected to a chemical analysis, phase analysis and microscopic examination using a high-temperature microscope. The results of microscopic examination were interpreted with reference to the chemical element composition and phase composition as well as in relation to their effect on the welding technique. The most important results obtained are presented below:

1. Welding with a BO low-hydrogen covered electrode leads to the formation of slag enriched in an amorphous phase having a significant effect on the welding technique. The increased viscosity of the amorphous silicate phases is responsible for better adhesion of liquid slag to the weld pool thus facilitating welding in difficult positions without slag flowing off and without the weld pool hanging down, which was observed during the test performed in the restricted PF position.

2. Due to the higher melting point of rutile electrode slags it is possible to use a welding technique employing an extended arc, facilitating welding in difficult positions. However, the high temperature of rutile slag solidification can be responsible for the confinement of gases inside the weld.

3. Slag formed while welding with a flux-cored wire (FCW) reveals the highest softening and melting points as well as the low temperature range between them. As a result, the slag solidifies faster and enables welding in difficult positions, e.g. in vertical progression, at high welding parameters, i.e. approximately 180 A.

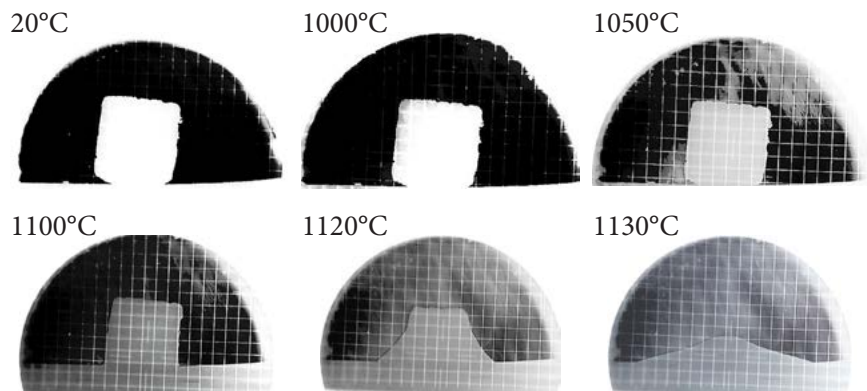


Fig. 5. Photographs of the BO specimen observed using a high-temperature microscope (1100°C-softening point, 1130°C-melting point).

## Acknowledgements

The authors wish to express their thanks to the Spaw-Projekt Company from Kraków for making the welds and to the “Instytut Łączenia Metali” Company from Kraków for financially supporting the research.

The work was partly financed with the statutory finances of the Faculty of Materials Science and Ceramics, AGH.

## References

- [1] Singh B., Khan Z.A., Siddiquee A.N.: Review on effect of flux composition on its behavior and bead geometry in submerged arc welding (SAW). *Journal of Mechanical Engineering Research*, 2013, vol. 5 (7), pp. 123-127.
- [2] Indacochea J.E., Blander M., Christensen N., Olson D.L.: Chemical reactions during Submerged Arc Welding with FeO-MnO-SiO<sub>2</sub> fluxes. *Metallurgical Transactions B*, 1985 vol. 16B, pp. 237-245.
- [3] Lau T., Weatherly G.C., Lean A.: The sources of oxygen and nitrogen contamination in submerged arc welding using CaO-Al<sub>2</sub>O<sub>3</sub> based fluxes. *Welding Research Supplement*, pp. 343-348, 1985.
- [4] Vaz C.T., Bracarense A.Q., Felizardo I., Pessoa E.C.: Impermeable low hydrogen covered electrodes: weld metal, slag, and fumes evaluation. *Journal of Materials Research and Technology*, 2012, no. 1 (2), pp. 64-70.
- [5] Jastrzębski R., Padula H., Trześniewski K., Jastrzębski A.: Steering algorithms of the root pass and the face for pressure high strength

- carbon steel and stainless steel pipes using the flux cored welding wire. 6<sup>th</sup> European Conference on Welding, Cutting and Joining Technologies EUROJOIN 6, Santiago de Compostela, 28-30.06.2006, pp. 363-373.
- [6] Jastrzębski R., Jastrzębski A.: Technika i technologia spawania elektrodą otuloną. Dozór Techniczny, 2013, no. 5, pp. 105-120.
- [7] Wyszomirski P., Galos K.: Surowce mineralne i chemiczne przemysłu ceramicznego. AGH Uczelniane Wydawnictwa Naukowo-Dydaktyczne, Kraków 2007.
- [8] Lech R.: Prędkość przemieszczania się granicy reakcyjnej podczas dysocjacji wapieni. Materiały Ceramiczne, 2006, no. 3, pp. 102-106.
- [9] Plessis J.D., Toit M.D., Pistorius P.C.: Control of diffusible weld metal hydrogen through flux chemistry modification, Welding Journal, 2007, no. 86, pp. 273-280.
- [10] Mitra U., Eagar T.W.: Slag-metal reactions during welding: Part I. Evaluation and reassessment of existing theories, Metallurgical Transactions B, 1991, vol. 22B, pp. 65-71.
- [11] Chai C.S., Eagar T.W.: Slag-metal equilibrium during submerged arc welding. Metallurgical Transactions B, 1981, vol. 12B, pp. 539-547.
- [12] Bang K., Park C., Jung H., Lee J.: Effects of flux composition on the element transfer and mechanical properties of weld metal in submerged arc welding. Metals and Materials International, 2009, no. 3, vol. 15, pp. 471-477.
- [13] Szczerba J.: Modyfikowane magnezjowe materiały ogniotrwałe. Ceramika, Polskie Towarzystwo Ceramiczne, Kraków 2007.
- [14] Jastrzębska I., Szczerba J., Madej D.: Wpływ rodzaju surowców magnezjowych na właściwości fizyczne i termomechaniczne betonów zasadowych. Materiały Ceramiczne, 2013, no. 3 (65), pp. 327-331.
- [15] Jastrzębska I., Szczerba J., Prorok R., Śnieżek E., Madej D.: Efekty procesu hydratacji ogniotrwałych betonów zasadowych. Logistyka, 2013, no. 4, pp. 174-184.
- [16] Niesyt M., Wyszomirski P., Galos R.: Analiza termiczna niektórych krajowych surowców dolomitowych-wybrane zagadnienia. Materiały Ceramiczne, 2011, no. 3 (63), pp. 619-625.
- [17] Eagar T.W.: Sources of weld metal oxygen contamination during submerged arc welding. Welding Research Supplement, 1978, pp. 76-80.
- [18] Chai C.S., Eagar T.W.: Slag metal reactions in binary CaF<sub>2</sub>-metal oxide welding fluxes. Welding Research Supplement, 1982, pp. 229-232.
- [19] Lau T., Weatherly G.C., Lean A. MC: Gas/Metal/Slag reactions in submerged arc welding using CaO-Al<sub>2</sub>O<sub>3</sub> based fluxes. Welding Research Supplement, 1986, pp. 31-38.
- [20] Datta I., Parekh M.: Filler metal flux basicity determination using the optical basicity index. Welding Research Supplement, 1989, pp. 68-76.
- [21] Terashima H., Tsuboi J.: Hydrogen in submerged arc weld metal produced with agglomerated flux. Welding Journal of Japan, 1976, no. 45, pp. 28-33.
- [22] Schwemer D.D., Olson D.L., Williamson D.L.: The relationship of weld penetration to the welding flux. Welding Research Supplement, 1979, pp. 153-160.
- [23] Hazzlet T.H.: Coatings ingredients influence on surface tension, arc stability and bead shapes. Welding Research Supplement, 1957, no. 36, pp. 18-23.
- [24] Olson D.L., Dixon R., Liby A. L.: Welding theory and practice. Materials Processing Theory and Practices, vol. 8, North-Holland Elsevier Science Publishing Company, Amsterdam 1990.
- [25] Tasak E., Jastrzębski A.: The influence of pulsation of the MIG arc on the structure of aluminium alloy welds. Welding International, Cambridge, 2012, vol. 25, no. 12, pp. 944-948.
- [26] Jastrzębski A., Tasak E.: Wpływ pulsacji łuku MIG na strukturę spoin stopów aluminium. Przegląd Spawalnictwa, 2009, no. 7-8, pp. 7-11.
- [27] Jastrzębski R., Śliwińska A., Jastrzębski A.: Szkolenie spawaczy w okresie rozwoju metod projektowania, technologii, materiałów i

- urządzeń. Przegląd Spawalnictwa, 2010, no. 5 (82), pp. 5-10.
- [28] Jastrzębski R., Cenin M., Jędrzejko J., Zieliński J., Jastrzębski K., Padula H.: Zastosowanie metody szkolenia spawaczy TKS do precyzyjnego wykonania przetopu i lica elektrodą zasadową w pozycjach przymusowych. Biuletyn Instytutu Spawalnictwa, 2005, no. 3, pp. 61-64.
- [29] Jastrzębski R., Pawlik (Jastrzębska) I.: Wady połączeń spawanych. Projektowanie i konstrukcje inżynierskie, 2011, no. 12 (51).
- [30] Jastrzębski R., Padula H., Zielińska M., Yalinkilicli B., Cenin M., Latala Z., Kościuszko T., Dexter M., Godniak M., Kaczor M.: Using space technic solution to design intelligent visual systems of industrial robots. Dokument MIS XII-1831-04.
- [31] Jastrzębski R., Mikuła J., Skarpetowski M., Żurek J.: Porównanie techniki spawania elektrodami otulonymi z drutami proszkowymi rutyłowymi i zasadowymi. Przegląd Spawalnictwa, 2011, no. 5 (83), pp. 45-47.